

UC San Diego

UC San Diego Previously Published Works

Title

Cortical and phase rim lesions on 7 T MRI as markers of multiple sclerosis disease progression.

Permalink

<https://escholarship.org/uc/item/0b0905hh>

Journal

Brain Communications, 3(3)

Authors

Treaba, Constantina
Conti, Allegra
Klawiter, Eric
et al.

Publication Date

2021

DOI

10.1093/braincomms/fcab134

Peer reviewed

BRAIN COMMUNICATIONS

Cortical and phase rim lesions on 7 T MRI as markers of multiple sclerosis disease progression

Constantina A. Treaba,^{1,2} Allegra Conti,³ Eric C. Klawiter,⁴ Valeria T. Barletta,^{1,2} Elena Herranz,^{1,2} Ambica Mehndiratta,¹ Andrew W. Russo,⁴ Jacob A. Sloane,⁵ Revere P. Kinkel,⁶ Nicola Toschi^{1,3,*} and Caterina Mainero^{1,2,*}

* These authors contributed equally to this work.

In multiple sclerosis, individual lesion-type patterns on magnetic resonance imaging might be valuable for predicting clinical outcome and monitoring treatment effects. Neuropathological and imaging studies consistently show that cortical lesions contribute to disease progression. The presence of chronic active white matter lesions harbouring a paramagnetic rim on susceptibility-weighted magnetic resonance imaging has also been associated with an aggressive form of multiple sclerosis. It is, however, still uncertain how these two types of lesions relate to each other, or which one plays a greater role in disability progression. In this prospective, longitudinal study in 100 multiple sclerosis patients (74 relapsing-remitting, 26 secondary progressive), we used ultra-high field 7-T susceptibility imaging to characterize cortical and rim lesion presence and evolution. Clinical evaluations were obtained over a mean period of 3.2 years in 71 patients, 46 of which had a follow-up magnetic resonance imaging. At baseline, cortical and rim lesions were identified in 96% and 63% of patients, respectively. Rim lesion prevalence was similar across disease stages. Patients with rim lesions had higher cortical and overall white matter lesion load than subjects without rim lesions ($P = 0.018-0.05$). Altogether, cortical lesions increased by both count and volume ($P = 0.004$) over time, while rim lesions expanded their volume ($P = 0.023$) whilst lacking new rim lesions; rimless white matter lesions increased their count but decreased their volume ($P = 0.016$). We used a modern machine learning algorithm based on extreme gradient boosting techniques to assess the cumulative power as well as the individual importance of cortical and rim lesion types in predicting disease stage and disability progression, alongside with more traditional imaging markers. The most influential imaging features that discriminated between multiple sclerosis stages (area under the curve \pm standard deviation = 0.82 ± 0.08) included, as expected, the normalized white matter and thalamic volume, white matter lesion volume, but also leukocortical lesion volume. Subarachnoid cerebrospinal fluid and leukocortical lesion volumes, along with rim lesion volume were the most important predictors of Expanded Disability Status Scale progression (area under the curve \pm standard deviation = 0.69 ± 0.12). Taken together, these results indicate that while cortical lesions are extremely frequent in multiple sclerosis, rim lesion development occurs only in a subset of patients. Both, however, persist over time and relate to disease progression. Their combined assessment is needed to improve the ability of identifying multiple sclerosis patients at risk of progressing disease.

- 1 Department of Radiology, Athinoula A. Martinos Center for Biomedical Imaging, Massachusetts General Hospital, Boston, MA 02129, USA
- 2 Harvard Medical School, Boston, MA 02115, USA
- 3 Department of Biomedicine and Prevention, University of Rome Tor Vergata, Rome 00133, Italy
- 4 Department of Neurology, Massachusetts General Hospital, Boston, MA 02115, USA
- 5 Department of Neurology, Beth Israel Deaconess Medical Center, Boston, MA 02215, USA
- 6 University of California San Diego, La Jolla, CA 92093, USA

Correspondence to: Caterina Mainero, MD, PhD
A.A. Martinos Center for Biomedical Imaging, Bldg. 149, 13th Street, Charleston, MA 02129, USA
E-mail: cmainero@mgh.harvard.edu

Keywords: multiple sclerosis; machine learning; MRI; cortical lesions; phase rim lesions

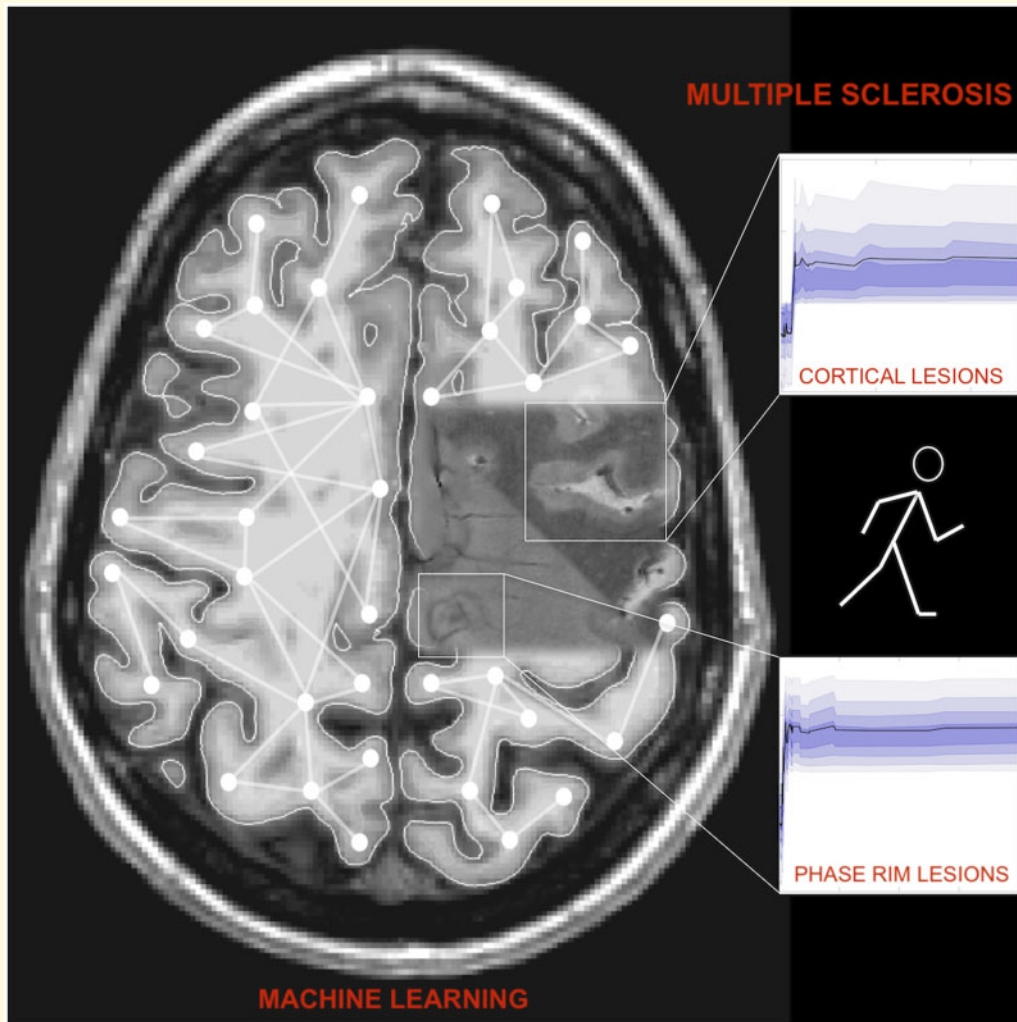
Received April 22, 2020.

© The Author(s) (2021). Published by Oxford University Press on behalf of the Guarantors of Brain. All rights reserved.

For permissions, please email: journals.permissions@oup.com

Abbreviations: AUC = area under the curve area from the receiver operating characteristic curve; EDSS = Expanded Disability Status Scale; RRMS = Relapsing-Remitting Multiple Sclerosis; SD = standard deviation; SHAP = Shapley Additive Explanations; SPMS = Secondary Progressive Multiple Sclerosis; XGBoost = Extreme Gradient Boosting

Graphical Abstract



Introduction

Multiple sclerosis is a demyelinating and neurodegenerative disease of the CNS and one of the most common causes of neurological disability in young adults in the Western world. The clinical course of multiple sclerosis is highly heterogeneous, with wide differences between patients in the rate of disease progression and disability accrual, in which the pathologic heterogeneity of multiple sclerosis lesion patterns is thought to play a role.^{1,2}

Magnetic resonance imaging is of paramount importance for early multiple sclerosis diagnosis, for monitoring treatment response in clinical practice and experimental trials and for investigating disease mechanisms. Although previous studies have described various MRI measures

predictive of long-term disability in different multiple sclerosis cohorts,^{3,4} a valid prediction of the clinical outcome has not yet been shown. Additionally, most findings are based on traditional statistical methods with limited generalizability and therefore often unknown true prediction power. As such, these measures need to be further improved and included into more robust statistical analysis to obtain robust markers of disability prediction.

Seven-tesla MRI has allowed the identification of novel radiological markers of multiple sclerosis pathology. Among these, slow expanding chronic white matter lesions, characterized by a paramagnetic rim on susceptibility-weighted images that colocalizes with activated iron-laden microglia,⁵⁻⁷ have been associated with remyelination failure⁸⁻¹⁰ and disability progression.^{6,7}

Neuropathological examinations consistently show that cortical demyelinating lesions are a hallmark of the disease progression.^{11–13} Cortical lesions, which show improved *in vivo* detection at 7-T,^{14–16} can develop from the earliest disease stages,^{17,18} correlate better with physical and cognitive impairment than white matter lesion load and cortical atrophy^{17,19,20} and independently predict disability progression.^{21–23} While the relationship between chronic rim and cortical lesions is still unknown, they may share common pathogenic mechanisms as microglia/macrophage activation is thought to underlie ongoing demyelination/repair failure at the edge of chronic rim lesions^{6,24} and some neuropathological^{25,26} and positron emission tomography data^{27,28} point to microglia involvement in the pathogenesis of cortical demyelination in multiple sclerosis.

Nevertheless, neither cortical nor chronic rim lesions are still routinely included in the clinical imaging assessment of multiple sclerosis disease burden.

In this longitudinal study, in a heterogeneous multiple sclerosis cohort, we aimed to characterize the prevalence, distribution and evolution of cortical and chronic rim lesions detected on susceptibility-weighted 7-T images. The main objective was to assess the cumulative power as well as individual importance of cortical and chronic rim lesions, alongside with traditional imaging markers, in predicting disease stage and disability progression using a modern machine learning algorithm based on extreme gradient boosting (XGBoost) techniques. We specifically selected this machine learning classifier algorithm as it has been shown that, while it supports both regression and classification predictive modelling problems,²⁹ it also performs extremely well with a population size of between 50 and 100.³⁰

Materials and methods

Study participants

From 2009 to 2019, we consecutively recruited 111 multiple sclerosis patients³¹ with either relapsing-remitting multiple sclerosis (RRMS, $n=74$) or secondary progressive multiple sclerosis (SPMS, $n=37$) who met the inclusion exclusion criteria (Fig. 1) along with 10 age-matched healthy control participants. Eleven participants' data were discarded due to motion artefacts. Clinical longitudinal data were obtained from 71 patients of whom 46 also had an MRI assessment at follow-up (Fig. 1).

The Institutional Review Board approved all study procedures and written informed consent in accordance with the Declaration of Helsinki was obtained from all participants before study enrolment.

MRI protocol and image analysis

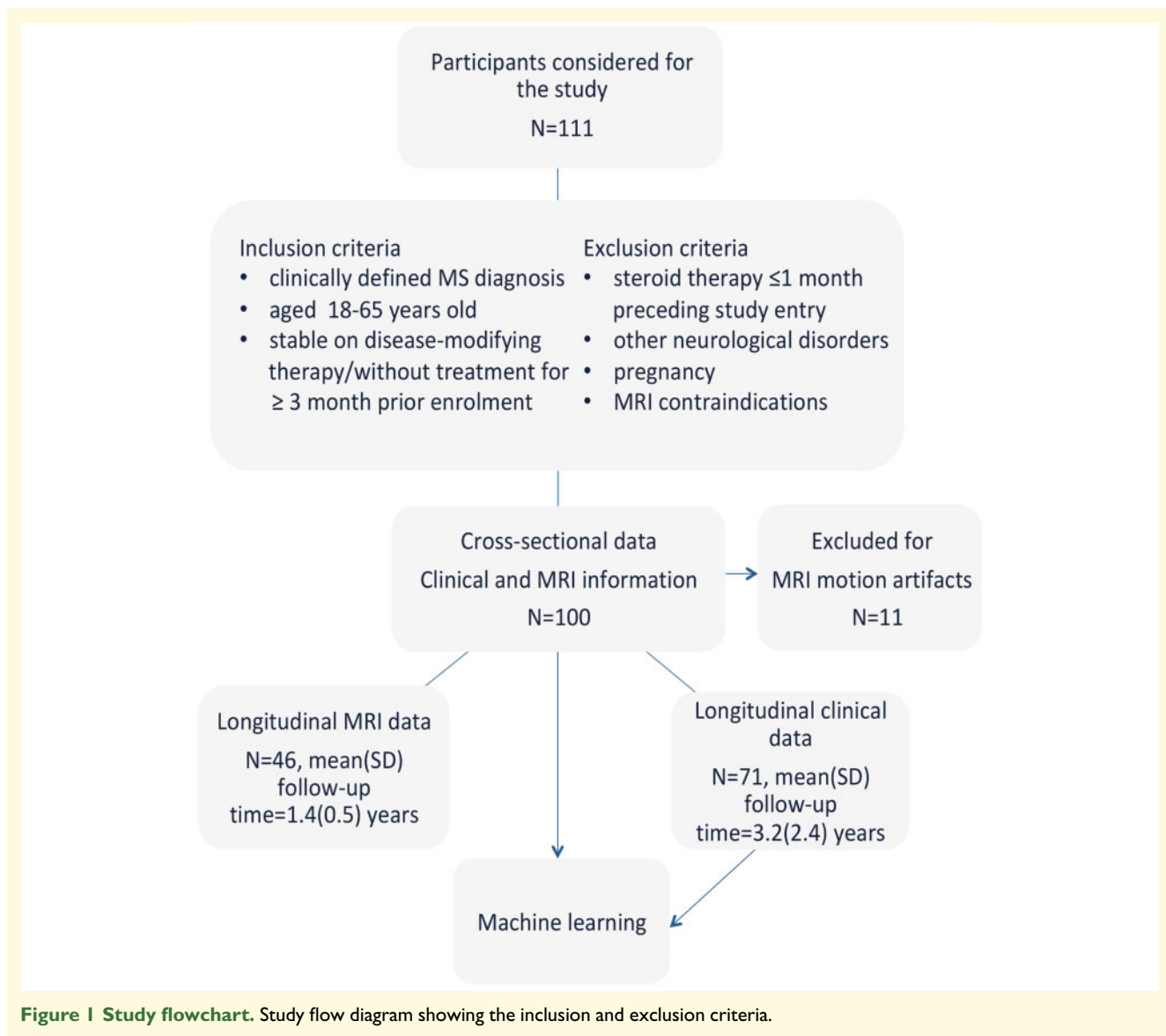
All study participants underwent two imaging sessions within a week on a 7-T and a 3-T MRI scanner using 32 channel coils to acquire: (i) 7-T two-dimensional fast low-angle shot T_2^* -weighted spoiled gradient-echo images to cover the supratentorial brain (repetition time/echo time [TR/TE] = 1700/21.8 msec, $0.33 \times 0.3 \times 1 \text{ mm}^3$ resolution) yielding magnitude and phase images for lesion segmentation and (ii) 3-T 3D T_1 -weighted scans [TR/inversion time (TI)/TE = 2530/1200 msec, $0.9 \times 0.9 \times 0.9 \text{ mm}^3$ resolution) for FreeSurfer reconstruction, cortical and subcortical segmentation and coregistration with 7-T data measurement (FreeSurfer Software version 5.3.0, 2013, <http://surfer.nmr.mgh.harvard.edu>; last accessed June 24, 2021). The topological defects in cortical surface reconstruction caused by the white matter and leukocortical lesions were accurately corrected using the in-painting method in all patients. Thalamic volume was computed as the sum of right and left thalami obtained by FIRST/FSL (<https://fsl.fmrib.ox.ac.uk/fsl/fslwiki/FIRST>; last accessed June 24, 2021) segmentation. Raw volumes were normalized to intracranial volume.

Lesion identification

Multiple sclerosis lesions were manually segmented on the magnitude 7-T T_2^* -weighted images using Slicer (version 4.4.0; <http://www.slicer.org>; last accessed June 24, 2021) by one radiologist (CAT), and one neurologist (CM) with experience in neuroimaging analysis working in agreement (for cortical lesion detection). Cortical lesions, designated to have a high intensity of at least 3 voxels across two consecutive slices were classified as intracortical if subpial¹¹ and confined to the cortex, or leukocortical if they also involved the white matter (Fig. 2). The reproducibility of cortical lesion quantification and the interrater agreement (kappa 0.69) were previously evaluated using up to 17 patients included in this study.^{14,32} The presence of rim lesions was assessed by the study radiologist (CAT) on 7-T phase images. A multiple sclerosis lesion was defined as 'rim lesion' when a susceptibility rim, a hypointense peripheral margin, was encircling an isointense to extralesional center³³ (Fig. 2).

The methodologic reliability was assessed by having a second rater (VB) identify rim lesions on 5 sample cases (inter-rater), while the first rater (CAT) reviewed the sample cases twice (intra-rater). In the analysis of lesion evolution, we defined a volume increase by 10% a lesion expansion, and a volume decrease by 10% a lesion reduction. If the change in a lesion was less than 10%, the lesion was considered steady.

FreeSurfer and FSL (version 5.0; <http://fsl.fmrib.ox.ac.uk>; last accessed June 24, 2021) tools were used to quantify the lesion counts and volumes. The presence of new



lesions was accounted for on a lesion-by-lesion basis, while the longitudinal lesion metrics were annualized using each patient's follow-up interval.

Disability measures

The clinical disability in multiple sclerosis patients was quantified by experienced neurologists (RPK, JAS, ECK), blinded to the MRI data, by using the Expanded Disability Status Scale (EDSS). All patients were evaluated with formal EDSS assessments, outside relapses, at least every 12 months and any EDSS increase of at least 1.0 point when the baseline EDSS was less than 6, or at least 0.5 points when the baseline EDSS was at least 6, was considered worsening if it persisted until the next annual visit or, in patients that were clinically followed for more than 1 year, if it was maintained for the last two consecutive annual visits.

Statistical analysis

Kolmogorov–Smirnov's test was used to assess normality. Differences in demographic and lesion load metrics between multiple sclerosis groups (i.e. RRMS versus SPMS, rim versus non-rim) were assessed using the Student's *t*-test for normally distributed data and the Mann–Whitney U-test (unrelated samples). Fisher's exact test was used for categorical data (sex, frequencies and treatment repartition). The Wilcoxon signed-rank test (related samples) evaluated the longitudinal changes in lesion volumes (non-normal data distributions). The differences in mean cortical thickness were assessed by analysis of covariance controlled for age and sex. Bivariate correlations were quantified using Spearman's rank correlation coefficient. Lin's concordance coefficient³⁴ was used to assess inter-rater and intra-rater reliability.

A two-tailed *P* value ≤ 0.05 as considered indicative of statistical significance. Statistical analysis was performed using SPSS version 25 (IBM) software.

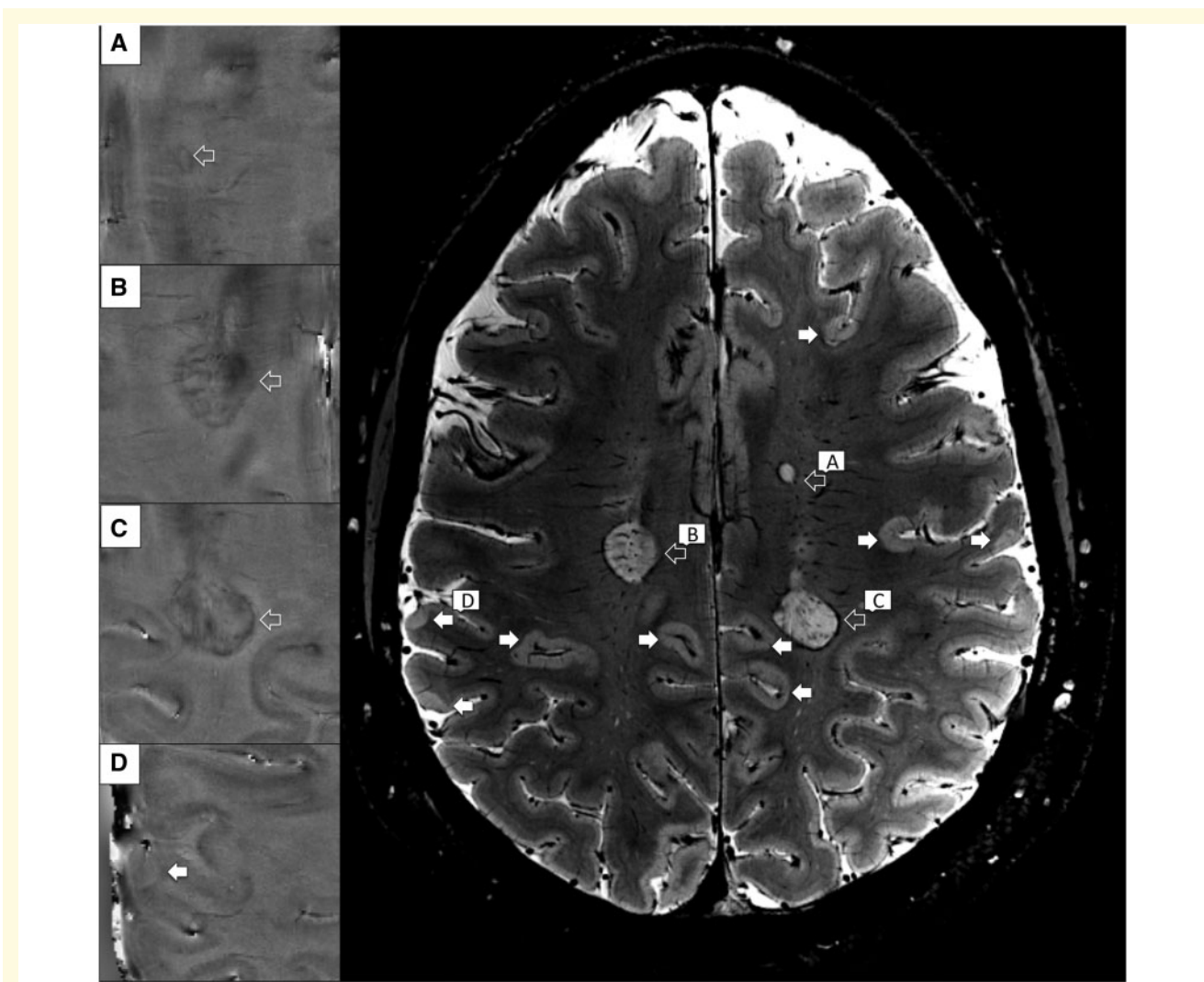


Figure 2 Cortical and rim lesions examples detected with 7-T T_2^* -weighted images. Cortical (white arrows) and white matter rim lesions (open arrows) as shown by axial 7-T T_2^* -weighted magnitude sequence in a 34 years old woman with relapsing remitting multiple sclerosis. Some lesions, involving either the white matter (A–C) or both white and cortical grey matter (D) are featuring a hypointense peripheral rim on phase images.

Classification analysis and feature importance

We used the XGBoost, an ensemble machine learning method based on decision trees, to generate prediction models for multiple sclerosis disease staging and neurological disability progression as well as to illustrate the importance of each feature included in the models. The predictors enclosed and comparatively assessed in the models (an overall total of 18, Table 1) were the potential novel radiological markers (cortical and rim lesion load MRI metrics) in conjunction with demographics and conventional MRI variables.

The complete dataset was split randomly into training (70%) and validation (30%) sets in a stratified manner. This splitting operation and successive procedures (see

below), was repeated 1000 times. For each training set, a genetic search pipeline with an evolutionary algorithm was used to explore hyperparameter values and their combinations³⁵ in a 5-fold cross-validation fashion, restricting the search to the XGBoost architecture.²⁹ XGBoost is a scalable end-to-end tree boosting system, which has shown state-of-the-art performances in a number of diverse machine learning applications and contests. After training, performance for each validation set was assessed by calculating the mean (across 1000 repetitions) and standard deviation (SD) of the area under the curve (AUC) from the receiver operating characteristic curve. Mean accuracy, sensitivity, and specificity alongside with the corresponding SDs across the 1000 optimized train/test splits were also calculated.

The contribution of each feature to the final prediction performance of the model was evaluated and compared

Table 1 List of variables used in machine learning algorithms to predict multiple sclerosis disease stage and neurological disability

Predictor variables
Rim presence or absence
Rim category (<3 or ≥4 rim lesions)
Rim lesion count
Rim lesion volume
Rimless white matter lesion count
Rimless white matter lesion volume
Intracortical lesion count
Intracortical lesion volume
Leukocortical lesion count
Leukocortical lesion volume
Normalized white matter volume
Normalized thalamic volume
Normalized subarachnoid CSF
Normalized intraventricular CSF
Cortical thickness
Age
Age at multiple sclerosis onset
Sex

by computing the Shapley Additive explanations (SHAP) values. These values are based on game-theoretical considerations and unify six existing methods for quantifying feature importance in a way which is more consistent with human reasoning relative to previous approaches.²⁹

At the dataset level, SHAP values allow to quantify average feature importance in terms of contribution to the prediction power of the model. In addition, we also analysed individual importance, i.e. how much a feature contributes to the classification of each separate individual. In turn, this allows investigating the association between feature importance and the value of the feature itself.

Treatment status was accounted for in the model that quantified the predictors of EDSS progression by regressing it out (binary variable treatment/no treatment) in each train split and by applying the computed transformation to the corresponding test/split. All classification analyses were implemented in Python 3.6 using the scikit-learn python module.³⁶

Data availability

The sharing of the data depends on Massachusetts General Hospital and Institutional Review Board policy and on the purpose of sharing the data (profit versus non-profit).

Results

Demographic and clinical variables

Demographic, clinical and MRI data of multiple sclerosis participants are shown in Table 2. At baseline, 37 of 100

patients were on first line therapy, 48 of 100 on second line therapy and 15 of 100 without therapy. Over a mean \pm SD of 3.2 years \pm 2.3, longitudinal EDSS scores were obtained in 71 patients. Approximately 24% (17 of 71) participants (9 with RRMS and 8 with SPMS) experienced EDSS progression at follow-up. By the end of follow-up, no RRMS entered in the secondary progressive phase.

Rim lesions at baseline

Sixty-three/100 patients had at least 1 rim lesion at baseline. Overall, 233/5161 white matter lesions (4.5%) and 14/1950 cortical lesions (0.7%) displayed a susceptibility rim on phase images. All cortical rim lesions were leukocortical (8 patients). All but two patients with leukocortical rim lesions presented white matter rim lesions as well. Owing to the limited number of leukocortical rim lesions, we included the leukocortical rim lesions in the same category with white matter rim lesions named hereafter as rim lesions.

The inter- and intra- rater agreement was substantial (Lin's concordance correlation coefficients of 0.98 and 0.99, respectively). No rim lesions were seen in the healthy control group, even if white matter lesions were seen in 6 healthy individuals (ranging from 1 to 7).

Across multiple sclerosis phenotypes, rim lesion prevalence [RRMS: 46 of 74 (62.1%) and SPMS: 17 of 26 (62.9%), $P=0.81$], count [RRMS: median 1 range (0, 14); SPMS: median 2 range (0, 33), $P=0.20$] and volume [RRMS: median 50, range (0, 9258 mm³), SPMS: 191 (0, 15 410 mm³), $P=0.18$] were similar.

No differences were detected in patients' age, disease duration, or in the number of which received a treatment when comparing multiple sclerosis patients according to presence or absence of rim lesions ($P=0.2-0.8$, Table 2).

Cortical lesions at baseline and relationship with rim lesions

A total of 1951 cortical lesions were identified in 96/100 MS patients (96%). As expected, cortical lesion count and volume was higher in SPMS patients relative to RRMS ($P<0.001$). All patients with rim lesions had also cortical lesions except for two patients (both RRMS). Overall, patients presenting with rim lesions had higher cortical and white matter lesion counts and volumes compared to patients without any identifiable rim lesions ($P=0.02-0.05$, Table 2).

Cortical and rim lesion loads were, however, moderately correlated ($[\rho=0.28, P=0.005]$ for counts and $[\rho=0.3, P=0.003]$ for volumes). No cortical lesions were found in healthy control participants.

Table 2 Demographics, clinical characteristics and MRI metrics of study participants at baseline

Parameter	Patients without rim lesions N = 37	Patients with rim lesions N = 63	P ^a	RRMS patients N = 74	SPMS patients N = 26	P ^b	Patients without EDSS progression N = 54	Patients with EDSS progression N = 17	P ^c
Gender (M:F)	6:31	18:45	0.23 ^d	14:60	10:16	0.06 ^d	11:43	3:14	1 ^d
Age (years), mean ± SD	44 ± 11	42 ± 9	0.22 ^e	41 ± 9	47 ± 9	0.009 ^e	41 ± 9	44 ± 8	0.24 ^e
RRMS:SPMS	28:9	46:17	0.82 ^d	—	—	—	44:10	9:8	0.03 ^d
Disease duration (years)	5 (0.1, 40)	8 (0.5, 40)	0.62 ^f	3 (0.1, 40)	19 (6, 40)	<0.001 ^f	3 (1, 40)	14 (1, 28)	0.007 ^f
EDSS	2 (0, 7.5)	2.5 (0, 8)	0.13 ^f	2 (0, 6)	4.7 (2, 8)	<0.001 ^f	2 (2, 7.5)	3 (0, 8)	0.2 ^f
Treatment	31	54	0.79 ^d	63	22	1 ^d	46	16	0.67 ^d
Rim lesion count	—	2 (1, 33)	—	1 (0, 14)	2 (0, 33)	0.19 ^f	1 (0, 29)	3 (0, 33)	0.03 ^f
Rim lesion volume, mm ³	—	298 (190, 15 410)	—	50 (0, 9258)	191 (0, 15 410)	0.18 ^f	48 (0, 4988)	347 (0, 15 410)	0.01 ^f
WM lesion count	22 (3, 264)	43 (5, 295)	0.02 ^f	22.5 (3, 171)	59.5 (14, 295)	<0.001 ^f	23 (3–204)	46 (5, 262)	0.12 ^f
WM lesion volume mm ³	639 (99, 52 154)	2699 (115, 22 456)	0.03 ^f	851 (99, 17 992)	8339 (212, 52 154)	<0.001 ^f	784 (72, 27 854)	3606 (200, 16 349)	0.07 ^f
Intracortical lesion count	3 (0, 37)	6 (0, 47)	0.04 ^f	4 (0, 32)	12.5 (0, 47)	0.002 ^f	5 (0, 47)	6 (0, 37)	0.49 ^f
Intracortical lesion volume, mm ³	144 (0, 1467)	247 (0, 3777)	0.09 ^f	163 (0, 3129)	574 (0, 3770)	<0.001 ^f	190 (0, 2103)	168 (0, 2737)	0.42 ^f
Leukocortical lesion count	1 (0, 98)	3 (0, 144)	0.08 ^f	2 (0, 34)	8.5 (0, 144)	<0.001 ^f	2 (0, 124)	3 (0, 144)	0.02 ^f
Leukocortical lesion volume, mm ³	65 (0, 4636)	203 (0, 9052)	0.04 ^f	84 (0, 3456)	578 (0, 9052)	<0.001 ^f	68 (0, 9052)	294 (0, 7157)	0.02 ^f
Normalized WM volume, mm ³	299 × 10 ⁻³	292 × 10 ⁻³	0.18 ^e	300 × 10 ⁻³	278 × 10 ⁻³	<0.001 ^e	298 × 10 ⁻³	283 × 10 ⁻³	0.04 ^e
Normalized thalamic volume, mm ³	(234 × 10 ⁻³ , 371 × 10 ⁻³)	(238 × 10 ⁻³ , 353 × 10 ⁻³)	0.70 ^f	(251 × 10 ⁻³ , 371 × 10 ⁻³)	(234 × 10 ⁻³ , 319 × 10 ⁻³)	<0.001 ^f	(245 × 10 ⁻³ , 353 × 10 ⁻³)	(238 × 10 ⁻³ , 327 × 10 ⁻³)	0.40 ^e
Normalized subarachnoid CSF volume, mm ³	631 × 10 ⁻⁵	614 × 10 ⁻⁵	0.70 ^f	638 × 10 ⁻⁵	554 × 10 ⁻⁵	<0.001 ^f	633 × 10 ⁻⁵	605 × 10 ⁻⁵	0.001 ^e
Normalized intraventricular CSF volume, mm ³	72 × 10 ⁻⁵	87 × 10 ⁻⁵	0.03 ^f	76 × 10 ⁻⁵	97 × 10 ⁻⁵	<0.001 ^f	76 × 10 ⁻⁵	99 × 10 ⁻⁵	0.02 ^f
Cortical thickness mean ± SD, mm	(39 × 10 ⁻⁵ , 203 × 10 ⁻⁵)	(50 × 10 ⁻⁵ , 183 × 10 ⁻⁵)	0.21 ^f	(39 × 10 ⁻⁵ , 203 × 10 ⁻⁵)	(59 × 10 ⁻⁵ , 183 × 10 ⁻⁵)	0.001 ^f	(41 × 10 ⁻⁵ , 131 × 10 ⁻⁵)	(45 × 10 ⁻⁵ , 193 × 10 ⁻⁵)	0.02 ^f
	(43 × 10 ⁻⁴ , 350 × 10 ⁻⁴)	(50 × 10 ⁻⁴ , 517 × 10 ⁻⁴)	0.53 ^g	(43 × 10 ⁻⁴ , 518 × 10 ⁻⁴)	(68 × 10 ⁻⁴ , 398 × 10 ⁻⁴)	0.06 ^g	(43 × 10 ⁻⁴ , 426 × 10 ⁻⁴)	(85 × 10 ⁻⁴ , 518 × 10 ⁻⁴)	0.83 ^g
	2.36 ± 0.12	2.38 ± 0.11		2.39 ± 0.11	2.32 ± 0.12		2.38 ± 0.11	2.37 ± 0.13	

EDSS, Expanded Disability Status Scale; RRMS, relapsing remitting multiple sclerosis; SPMS, secondary progressive multiple sclerosis; WM, white matter; Variables are summarized as median (range) if not otherwise noted.

^aFor comparisons between the group of multiple sclerosis patients with rim lesions versus the group of multiple sclerosis patients without rim lesions.

^bFor comparisons between RRMS and SPMS patients.

^cFor comparisons between patients with and without EDSS progression.

^dP value by Fisher exact test (two-sided).

^eP value by unpaired two-tailed t-test (equal variances not assumed).

^fP value by Mann-Whitney U-test (two-tailed).

^gP value by analysis of covariance adjusted for age and gender and corrected for multiple comparisons (Bonferroni).

Longitudinal assessment shows distinct patterns of lesion evolution in the cortex and in white matter

Longitudinal MRI data were obtained in 46 patients (36 RRMS and 10 SPMS) over a mean \pm SD of 1.4 years \pm 0.5 (Supplementary Table 1). Overall, 2342 white matter lesions and 1024 cortical lesions were identified at baseline. In 31/46 subjects who had longitudinal MRI, 149 lesions were surrounded by a susceptibility rim. All lesions detected at baseline persisted at follow-up, while 174 new lesions (60 white matter and 114 cortical) developed during the observation period in 38/46 (82.6%) patients. No new rim lesion was detected at follow-up. We were unable to detect differences in the incidence of new white matter or cortical lesions in patients with or without rim lesions [new white matter lesions: 61% (19/31) versus 53% (8/

15), $P=0.75$ and new cortical lesions: 77% (24/31) versus 53% (8/15), $P=0.17$, respectively]. Similarly, the annual rate of new cortical and white matter lesions was about the same (1 ± 1 versus 2 ± 2.9 , $P=0.4$ for cortical and 0.7 ± 1.1 versus 0.9 ± 1.5 , $P=0.9$ for white matter lesions) regardless of the presence of rim lesions.

Looking at individual rim lesions' evolution, we found that the volume was stable in 44.3% (66/149) of lesions, shrank in 24.8% (37/149) of them while exhibited an ongoing increase in 30.9% (46/149%) of lesions (Supplementary Fig. 1). Taken altogether, there was a slight increase in their volume at follow-up (mean \pm SD; 834 ± 2491 mm³ versus 838 ± 2534 mm³, $P=0.027$, Fig. 3). On contrary, the rimless white matter lesion volume decreased (3002 ± 4360 mm³ versus 2956 ± 4148 mm³, $P=0.016$, Fig. 3) despite the addition of the new lesions.

Looking at each patient lesion evolution we observed that the cortical lesion volume increased in 20/46

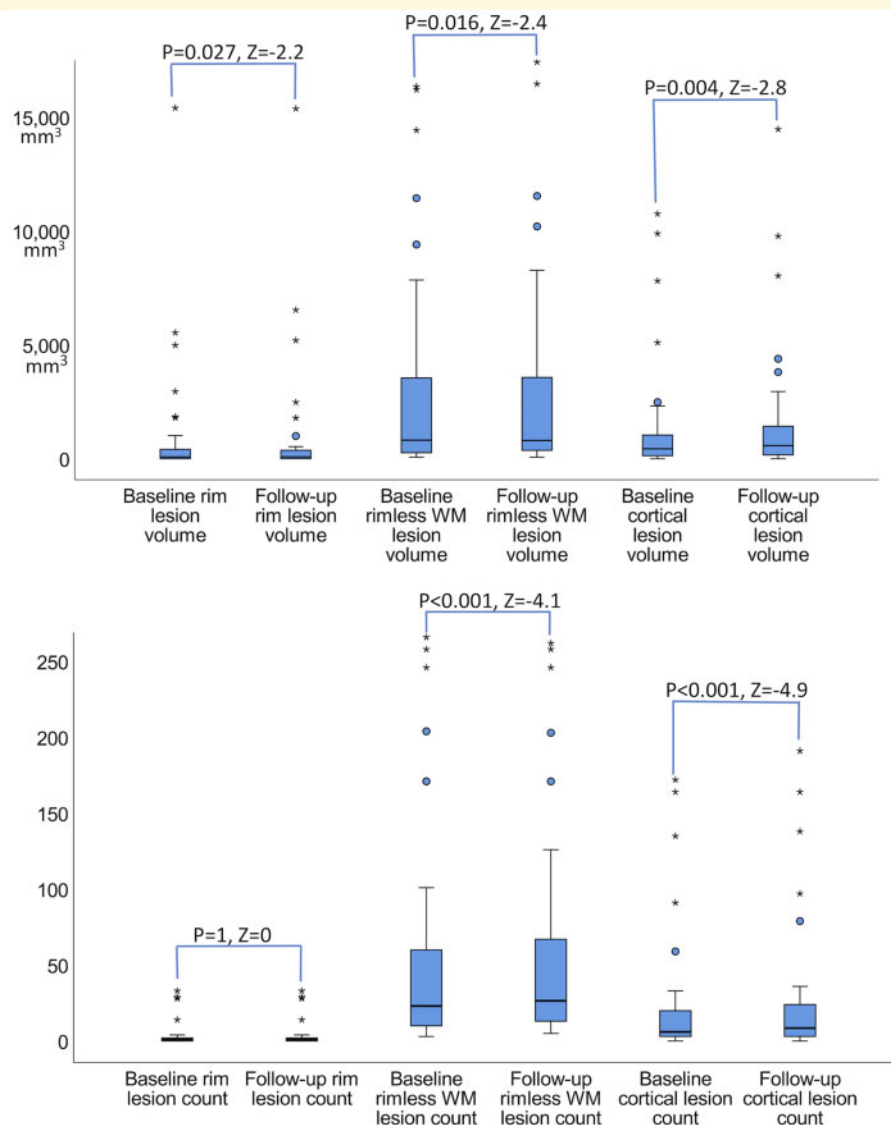


Figure 3 Boxplots summarizing the longitudinal changes of multiple sclerosis lesions in 46 patients. The cortical and rim lesion volumes increased over time while the rimless white matter volume decreased (A) despite the new white matter lesion formation (B) in multiple sclerosis patients. P and Z -statistic values by Wilcoxon signed rank test (related samples, two-tailed).

(43.5%) patients. Among those, 14/20 (70%) patients also presented rim lesions, but an associated increase in the rim lesion volume was only noted in 3/14 (21.4%) patients. Overall, the volume of cortical lesions increased from $1269 \pm 2397 \text{ mm}^3$ to $1460 \pm 2757 \text{ mm}^3$, $P = 0.004$.

Disease stages is predicted by both traditional metrics of disease burden and cortical lesions

The model built for predicting disease stage achieved a mean \pm SD AUC value of 0.82 ± 0.08 with a sensitivity of 0.78 ± 0.09 , an accuracy of 0.77 ± 0.07 and a specificity of

0.73 ± 0.17 . Figure 4 summarizes the features' importance ranking for this model, where larger values indicate a larger contribution to the final prediction. The top six most important features for classifying multiple sclerosis patients into the different disease stages (RRMS and SPMS) included the normalized volumes of the white matter, thalamus, as well as rimless white matter and leukocortical lesion volumes, rimless white matter lesion count and the normalized intraventricular CSF.

Interestingly, the importance of the counts of cortical and rim lesions as well as of the intracortical and rim lesion volumes in prediction in the disease course prediction was small, being ranked below the sixth position.

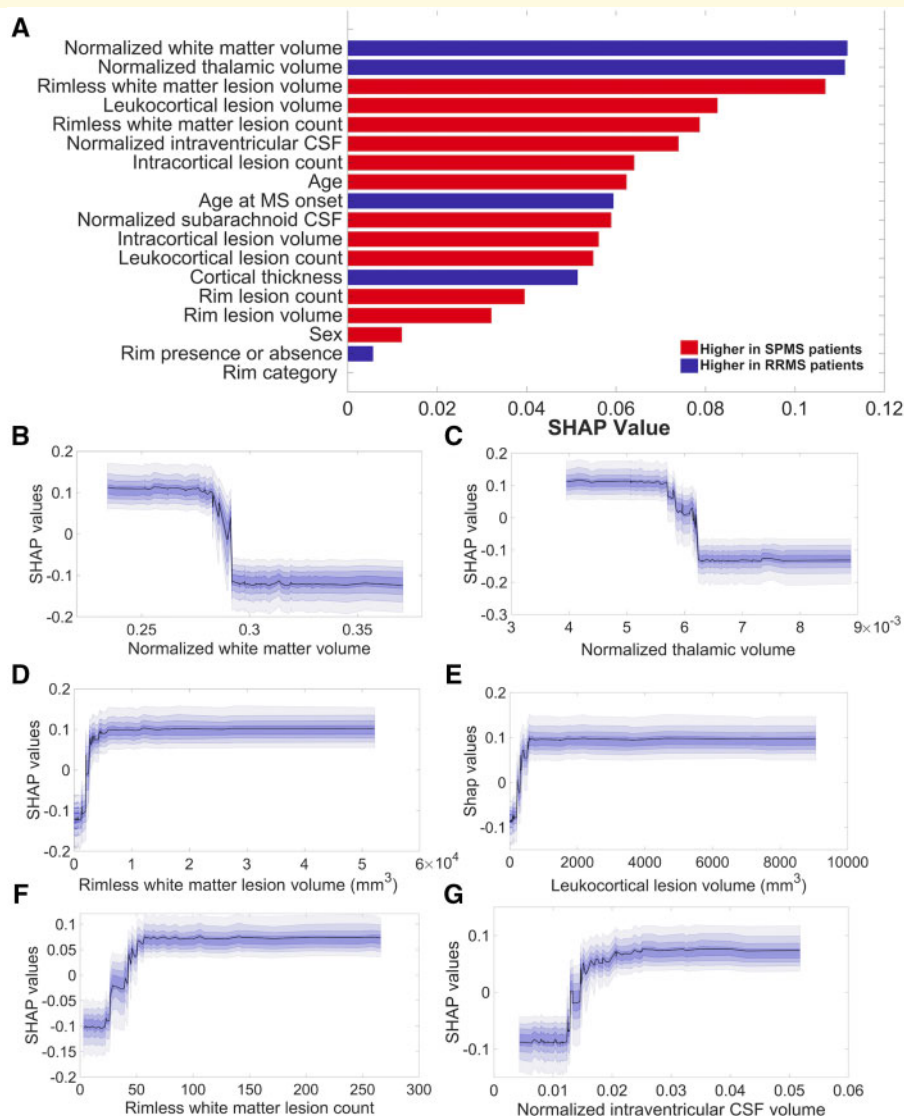


Figure 4 Machine learning in disease stage prediction in a cohort of 100 multiple sclerosis patients. The resulting SHAP features ranking (**A**) derived from XGBoost model lists, in descending order, starting with the most significant features in disease stage prediction. The model reached a mean \pm SD area under the curve value of 0.82 ± 0.08 , a sensitivity of 0.78 ± 0.09 , an accuracy of 0.77 ± 0.07 and a specificity of 0.73 ± 0.17 . The partial SHAP dependence plots (median and confidence intervals across repetitions, **B–G**) are shown for the top six most important features for classifying multiple sclerosis patients in different disease stages [relapsing-remitting multiple sclerosis (RRMS) and secondary progressive multiple sclerosis (SPMS)].

Table 3 The values of the top-ranked features that exert a maximal impact on feature's importance in the predictive models

Parameter	Predictor	Mean value (range), mm ³
MS phenotypes	Normalized WM volume	0.287 (0.282–0.292)
	Normalized thalamic volume	0.0059 (0.0057–0.0062)
	Rimless WM lesion volume	3000 (1090–4910)
	Leukocortical lesion volume	327 (70–584)
	Rimless WM lesion volume	38.5 (22–55)
EDSS progression	Normalized intraventricular CSF volume	0.016 (0.012–0.021)
	Normalized subarachnoid CSF volume	0.00089 (0.00086–0.00092)
	Rim lesion volume	213 (79–347)
	Leukocortical lesion volume	247.8 (202.6–293)
	Normalized WM volume	0.2904 (0.2875–0.2951)
	Normalized intraventricular CSF volume	0.0136 (0.0112–0.0155)
	Rim lesion count	2 (1–3)

As shown by the partial dependence plots (Fig. 4), the importance of each feature in the model's prediction remains the same with the increase of the feature's value up to a certain narrow interval (Table 3), where its importance will either escalate or decline and successively remain stable.

Cortical pathology and rim lesions are main predictors of disability progression

The model's ability to predict neurological disability progression reached an AUC value of 0.69 ± 0.11 , a sensitivity of 0.71 ± 0.10 , an accuracy of 0.68 ± 0.09 and a specificity of 0.58 ± 0.21 . The foremost predictors of EDSS progression were the normalized subarachnoid CSF volume, the leukocortical lesion volumes and the rim lesion volume. They were followed by the normalized volumes of white matter and intraventricular CSF as well as by rim lesion count (Fig. 5), which came in sixth. The partial dependence plots of the top six features (Fig. 5) displayed the same trends as the predictors of the multiple sclerosis stages. The intervals in which the changes in the feature's importance appeared alongside the mean intervals' values are listed in Table 3.

Discussion

Using susceptibility-based brain sequences at ultra high field MRI in a heterogeneous cohort of 100 multiple sclerosis cases, we demonstrated that lesions characterized by a susceptibility rim are relatively frequent (up to ~60% of patients) and occur mostly within the white matter, with a similar incidence across disease phenotypes. In contrast to rimless white matter lesions, which tend to reduce their volume over time despite the occurrence of new ones, rim lesions persist and progressively expand. We also found that in patients with multiple sclerosis

cortical lesions are even more frequent and show a faster and greater rate of progression than rim lesions.

We applied machine-learning algorithms to assess the cumulative power and individual importance of cortical and rim lesion types, alongside with traditional imaging markers of disease burden, in predicting disease stage and disability progression. We found that cortical and rim lesion types were main predictors of EDSS progression (over a mean of 3.2 years and along with the normalized subarachnoid CSF volume). However, their importance was lower in discriminating between different multiple sclerosis disease stages.

The finding of a susceptibility rim at the edge of some chronic lesions located in white matter was acknowledged in certain multiple sclerosis patients^{24,37–39} being linked to activated iron-laden microglia^{5,6,40} and with an expanding lesion pattern.^{5,41} While the substrate of cortical lesions seems to also involve activated microglial cells²⁶ most likely associated to meningeal and/or perivascular inflammation^{25,42} a relationship between cortical and rim-type white matter lesions can't be excluded. Furthermore, a microglial susceptibility rim might be present in some cortical lesions¹⁵ as well.

Our results demonstrate that cortical and rim lesions evolve in the same way by increasing their volume over time, but the increase of the rim and cortical lesion volumes seem to be independent of each other as they do not necessarily share the same time frame except in a few cases. In addition, the frequency of rim lesion development appears to be lower than that of the cortical or white matter rimless lesions, since over a mean of 3.2 years, we identified 176 new cortical and rimless white matter lesions but no new rim lesions. Since previous data found that nascent rim lesions could be identified within a follow-up time extending up to 7 years,⁴¹ it is likely that the rim lesion formation requires more time than the interval we followed our patients.

While it remains still unknown why the rim lesions only develop in some patients, our results show that the patients harbouring rim lesions concurrently exhibit a

higher white matter and cortical lesion load relative to the patients without rim lesions, possibly pointing to an abnormal microglia response to perturbations in the CNS milieu.⁴³ Nevertheless, our data also indicate that the volume of the rimless white matter lesions decrease over time, despite the addition of the new white matter lesions, most likely due to glial scar formation.⁴⁴

While the transition from RRMS to SPMS is difficult to define clinically, the use of an advanced machine learning method, allowed us to distinguish between RRMS and SPMS patients with a high accuracy. As model-free machine learning methods do not depend on a priori information and have minimal statistical assumptions, they outperform regression-based statistical techniques on complex data sets with a large number of

features⁴⁵ and avoid multicollinearity problems.⁴⁶ Besides, the state-of-the-art version of boosted trees (XGBoost) performs extremely well even with a relatively small sample size³⁰ and in our case, the number of patients was one order of magnitude larger than the number of features, hence limiting overfitting in itself. We also repeatedly random stratified 70/30 test (unseen) training split not 1 but 1000 times in order to reduce random-seed induced bias and estimate confidence intervals for our results. Overfitting was, thus, reduced to a minimum in our study, suggesting that our results can be considered generalizable to out-of sample instances, as opposed to the results of conventional regression methods.

Not surprisingly, the highest ranked predictors of the disease stage identified were the traditional MRI metrics

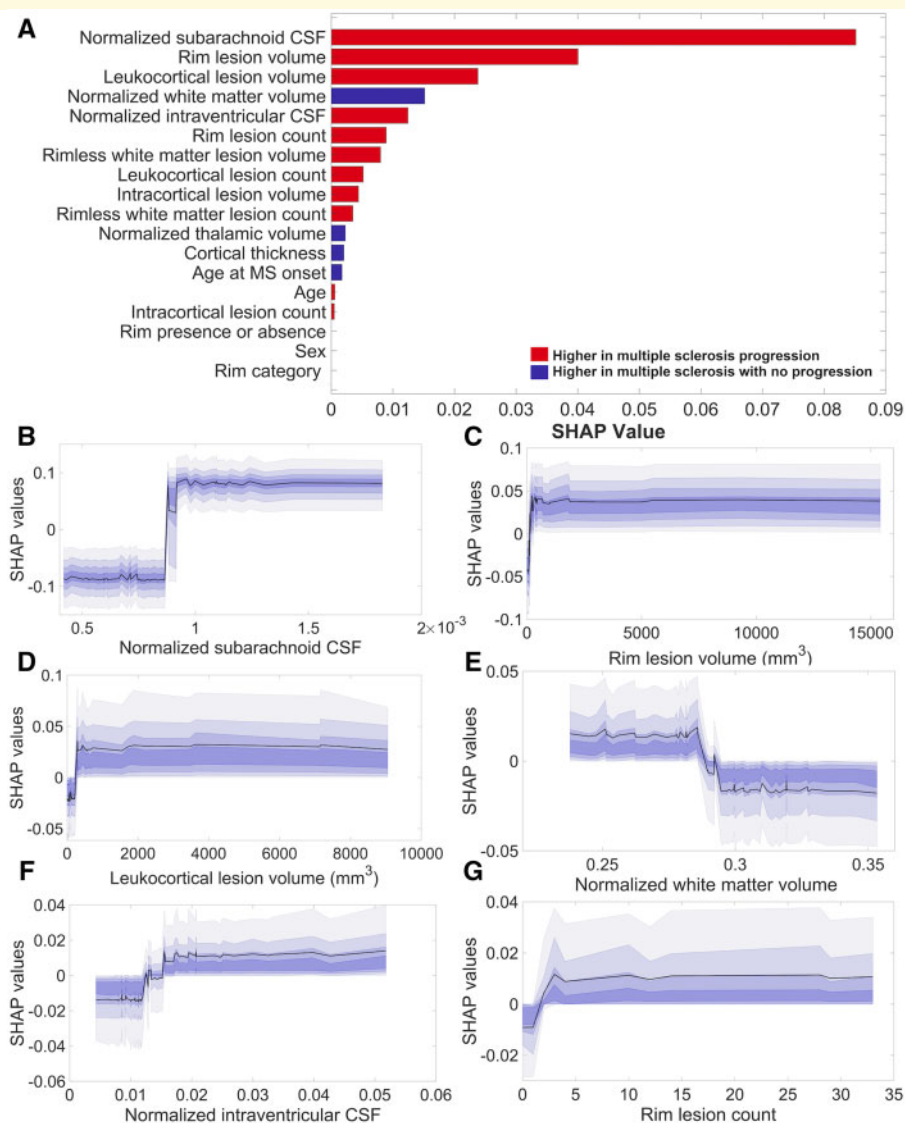


Figure 5 Influential predictors of neurological disability progression in multiple sclerosis. The resulting SHAP features ranking (A) derived from XGBoost model lists, in descending order, starting with the most significant features in the prediction of neurological disability progression in multiple sclerosis. The model reached a mean \pm SD area under the curve value of 0.69 ± 0.11 , a sensitivity of 0.71 ± 0.10 , an accuracy of 0.68 ± 0.09 and a specificity of 0.58 ± 0.21 . The partial SHAP dependence plots (median and confidence intervals across repetitions, B–G) are shown for the top six contributors to the prediction.

of white matter and thalamic atrophy and the rimless white matter lesion volume.

Even if the rimless white matter lesion volume tends to contract as disease progresses,^{47,48} SPMS patients still show higher rimless white matter lesion volume relative to RRMS. Leukocortical lesion volume came in fourth, likely due to the greater leukocortical lesion load demonstrated in patients with SPMS relative to RRMS.^{23,49}

Intracortical lesions were lower than the leukocortical lesion type in the rankings. This could potentially be related to the underestimation of the subpial lesion load with MRI, but could be also explained by the presence of intracortical demyelination very early in the course of multiple sclerosis.^{18,50} Rim lesions (both counts and volumes) were also ranked low as predictors for discriminating multiple sclerosis stages, pointing towards the fact that the presence of rim within the white matter lesions is a frequent encounter in all multiple sclerosis disease stages, being even associated with lesion formation⁵¹. Alternatively, the rim disappearance over time⁴¹ might also play a role in the low ranking detected.

Using the XGBoost and SHAP approaches, we also identified the normalized subarachnoid CSF volume, and the rim and the leukocortical lesion volumes as the main predictors of EDSS change at follow-up. While the first denotes the presence of cortical atrophy, the other two are related to lesion types that are not currently included as imaging outcome measurements of clinical decision support or treatment efficacy target.

While previous studies have linked the persistent rim lesions⁶ and the presence of four or more rim lesions⁷ in multiple sclerosis patients with a poor outcome, our results show that it is the rim lesion volume that matters more (although it is not the only factor that contributes) to an increase in EDSS over time.

Furthermore, the importance of rim lesion volume in the EDSS prediction steeply increases until the rim lesion volume value reaches a certain and rather narrow interval, and afterwards remains stable and continues to relate to EDSS changes.

Leukocortical lesions ranked high, being the third predictor of disability progression, possibly due to their destructive potential^{52,53} and great discoverability at 7-T.¹⁶

In contrast, intracortical lesions' volume ranked low, although still in the top ten predictors of EDSS progression, possibly related to the particularities of our patient's cohort (comprised by many early RRMS patients) and the suboptimal detection of subpial lesions.¹⁶

Interestingly, we have also found that lesion accumulation occurs more rapidly for cortical as compared to rim type lesions. As accumulation of the new lesions in the cortex has been consistently shown to contribute to their volume increase, tracking their development and evolution could be particularly important for clinical trials with reduced observation times.

This study had several limitations. First, since even 7-T MRI fails to detect a large number of intracortical lesions in multiple sclerosis,^{15,16} their contribution to neurologic disability progression has certainly been underrated.

Second, although the AUC value for predicting the neurological disability progression (0.69) was not ideal, it still approached discrimination. Third, in this work neither the association between rim and the spinal cord lesions nor the contribution of spinal cord lesions to neurologic disability⁵⁴ have been investigated. This was due to the fact that spinal cord MRI data were acquired only in a limited number of patients in this cohort. Fourth, the disability progression was assessed only by means of EDSS.

Future studies will address such aspects by including additional disability measures besides a larger population size, in an effort to contribute to the development of a clinically usable prognostic tool.

Conclusion

Despite limitations, our study demonstrated that rim and cortical lesions in patients with multiple sclerosis share common important features: they are frequent, persistent, progress over time and contribute independently to disability progression.

As such, the combined evaluation of rim and cortical lesion volumes in multiple sclerosis might result in an improved ability to distinguish the patients susceptible to experience a progression of the neurological disability and could influence the therapeutic decision.

Supplementary material

Supplementary material is available at *Brain Communications* online.

Acknowledgements

We would like to thank Mary Foley for her technical assistance with MRI scanning, all the subjects who participated in the study and the anonymous reviewers for their valuable feedback.

Funding

This work was supported by grants from the National Multiple Sclerosis Society (NMSS 4281-RG-A1, NMSS RG 4729A2/1 and NMSS RG 1802-30468), National Institutes of Health R01NS078322-01-A1, and United States Army W81XWH-13-1-0122. E. H. has received research support by the NMSS fellowship FG-1507-05459.

Competing interests

E.C.K. has received consulting fees from Alexion, Biogen, EMD Serono, Genentech and medDay, and has received research funding from Abbvie, Biogen, EMD Serono, Genzyme and Genentech/Roche. All other authors report no competing interests.

References

1. Frischer JM, Weigand SD, Guo Y, et al. Clinical and pathological insights into the dynamic nature of the white matter multiple sclerosis plaque. *Ann Neurol*. 2015;78(5):710–721.
2. Luchetti S, Fransen NL, van Eden CG, Ramaglia V, Mason M, Huitinga I. Progressive multiple sclerosis patients show substantial lesion activity that correlates with clinical disease severity and sex: A retrospective autopsy cohort analysis. *Acta Neuropathol*. 2018;135(4):511–528.
3. Ontaneda D, Fox RJ. Imaging as an outcome measure in multiple sclerosis. *Neurotherapeutics*. 2017;14(1):24–34.
4. Moccia M, de Stefano N, Barkhof F. Imaging outcome measures for progressive multiple sclerosis trials. *Mult Scler*. 2017;23(12):1614–1626.
5. Dal-Bianco A, Grabner G, Kronnerwetter C, et al. Slow expansion of multiple sclerosis iron rim lesions: Pathology and 7 T magnetic resonance imaging. *Acta Neuropathol*. 2017;133(1):25–42.
6. Absinta M, Sati P, Schindler M, et al. Persistent 7-tesla phase rim predicts poor outcome in new multiple sclerosis patient lesions. *J Clin Invest*. 2016;126(7):2597–2609.
7. Absinta M, Sati P, Masuzzo F, et al. Association of chronic active multiple sclerosis lesions with disability in vivo. *JAMA Neurol*. 2019;76(12):1474.
8. Lassmann H, Raine CS, Antel J, Prineas JW. Immunopathology of multiple sclerosis: Report on an international meeting held at the Institute of Neurology of the University of Vienna. *J Neuroimmunol*. 1998;86(2):213–217.
9. Popescu BF, Lucchinetti CF. Pathology of demyelinating diseases. *Annu Rev Pathol*. 2012;7:185–217.
10. Kuhlmann T, Ludwin S, Prat A, Antel J, Brück W, Lassmann H. An updated histological classification system for multiple sclerosis lesions. *Acta Neuropathol*. 2017;133(1):13–24.
11. Bo L, Vedeler CA, Nyland HI, Trapp BD, Mork SJ. Subpial demyelination in the cerebral cortex of multiple sclerosis patients. *J Neuropathol Exp Neurol*. 2003;62(7):723–732.
12. Kutzelnigg A, Lassmann H. Cortical demyelination in multiple sclerosis: A substrate for cognitive deficits? *J Neurol Sci*. 2006;245(1-2):123–126.
13. Kutzelnigg A, Faber-Rod JC, Bauer J, et al. Widespread demyelination in the cerebellar cortex in multiple sclerosis. *Brain Pathol*. 2007;17(1):38–44.
14. Mainero C, Benner T, Radding A, et al. In vivo imaging of cortical pathology in multiple sclerosis using ultra-high field MRI. *Neurology*. 2009;73(12):941–948.
15. Pitt D, Boster A, Pei W, et al. Imaging cortical lesions in multiple sclerosis with ultra-high-field magnetic resonance imaging. *Arch Neurol*. 2010;67(7):812–818.
16. Kilsdonk ID, Jonkman LE, Klaver R, et al. Increased cortical grey matter lesion detection in multiple sclerosis with 7 T MRI: A post-mortem verification study. *Brain*. 2016;139(5):1472–1481.
17. Mainero C, Louapre C, Govindarajan ST, et al. A gradient in cortical pathology in multiple sclerosis by in vivo quantitative 7 T imaging. *Brain*. 2015;138(4):932–945.
18. Granberg T, Fan Q, Treaba CA, et al. In vivo characterization of cortical and white matter neuroaxonal pathology in early multiple sclerosis. *Brain*. 2017;140(11):2912–2926.
19. Harrison DM, Roy S, Oh J, et al. Association of cortical lesion burden on 7-T magnetic resonance imaging with cognition and disability in multiple sclerosis. *JAMA Neurol*. 2015;72(9):1004–1012.
20. Nielsen AS, Kinkel RP, Madigan N, Tinelli E, Benner T, Mainero C. Contribution of cortical lesion subtypes at 7T MRI to physical and cognitive performance in MS. *Neurology*. 2013;81(7):641–649.
21. Calabrese M, Rocca MA, Atzori M, et al. A 3-year magnetic resonance imaging study of cortical lesions in relapse-onset multiple sclerosis. *Ann Neurol*. 2010;67(3):376–383.
22. Calabrese M, Poretto V, Favaretto A, et al. Cortical lesion load associates with progression of disability in multiple sclerosis. *Brain*. 2012;135(10):2952–2961.
23. Treaba CA, Granberg TE, Sormani MP, et al. Longitudinal characterization of cortical lesion development and evolution in multiple sclerosis with 7.0-T MRI. *Radiology*. 2019;291(3):740–749.
24. Bagnato F, Hametner S, Yao B, et al. Tracking iron in multiple sclerosis: A combined imaging and histopathological study at 7 Tesla. *Brain*. 2011;134(Pt 12):3602–3615.
25. Magliozzi R, Howell OW, Reeves C, et al. A Gradient of neuronal loss and meningeal inflammation in multiple sclerosis. *Ann Neurol*. 2010;68(4):477–493.
26. Lucchinetti CF, Popescu BF, Bunyan RF, et al. Inflammatory cortical demyelination in early multiple sclerosis. *N Engl J Med*. 2011;365(23):2188–2197.
27. Politis M, Giannetti P, Su P, et al. Increased PK11195 PET binding in the cortex of patients with MS correlates with disability. *Neurology*. 2012;79(6):523–530.
28. Herranz E, Gianni C, Louapre C, et al. Neuroinflammatory component of gray matter pathology in multiple sclerosis. *Ann Neurol*. 2016;80(5):776–790.
29. Chen T, Guestrin C. XGBoost: A scalable tree boosting system. *In: KDD'16: Proceedings of the 22nd ACM SIGKDD International Conference on Knowledge Discovery and Data Mining*. San Francisco; 2016. 785–794.
30. Floares GA, Fm OD, Cipariu A, Calin GA, Manolache FB. The smallest sample size for the desired diagnosis accuracy. *Int J Oncol Cancer Ther*. 2017;2:13–19.
31. Polman CH, Reingold SC, Banwell B, et al. Diagnostic criteria for multiple sclerosis: 2010 revisions to the McDonald criteria. *Ann Neurol*. 2011;69(2):292–302.
32. Nielsen AS, Kinkel RP, Tinelli E, Benner T, Cohen-Adad J, Mainero C. Focal cortical lesion detection in multiple sclerosis: 3 Tesla DIR versus 7 Tesla FLASH-T2. *J Magn Reson Imaging*. 2012;35(3):537–542.
33. Yao B, Bagnato F, Matsuura E, et al. Chronic multiple sclerosis lesions: Characterization with high-field-strength MR imaging. *Radiology*. 2012;262(1):206–215.
34. Lin LI. A concordance correlation coefficient to evaluate reproducibility. *Biometrics*. 1989;45(1):255–268.
35. Le TT, Fu W, Moore JH. Scaling tree-based automated machine learning to biomedical big data with a feature set selector. *Bioinformatics*. 2020;36(1):250–256.
36. Pedregosa F, Varoquaux G, Gramfort A, et al. Scikit-learn: Machine learning in Python. *J Mach Learn Res*. 2011;(12):2825–2830.
37. Hammond KE, Metcalf M, Carvajal L, et al. Quantitative in vivo magnetic resonance imaging of multiple sclerosis at 7 Tesla with sensitivity to iron. *Ann Neurol*. 2008;64(6):707–713.
38. Mehta V, Pei W, Yang G, et al. Iron is a sensitive biomarker for inflammation in multiple sclerosis lesions. *PLoS One*. 2013;8(3):e57573.
39. Yao B, Ikonomidou VN, Cantor FK, Ohayon JM, Duyn J, Bagnato F. Heterogeneity of multiple sclerosis white matter lesions detected with T2-weighted imaging at 7.0 Tesla. *J Neuroimaging*. 2015;25(5):799–806.
40. Kaunzner UW, Kang Y, Zhang S, et al. Quantitative susceptibility mapping identifies inflammation in a subset of chronic multiple sclerosis lesions. *Brain*. 2019;142(1):133–145.
41. Dal-Bianco A, Grabner G, Kronnerwetter C, et al. Long-term evolution of multiple sclerosis iron rim lesions in 7 T MRI. *Brain*. 2021;144(3):833–847.
42. Magliozzi R, Howell O, Vora A, et al. Meningeal B-cell follicles in secondary progressive multiple sclerosis associate with early onset of disease and severe cortical pathology. *Brain*. 2007;130(Pt 4):1089–1104.
43. Deczkowska A, Amit I, Schwartz M. Microglial immune checkpoint mechanisms. *Nat Neurosci*. 2018;21(6):779–786.
44. Popescu BF, Pirko I, Lucchinetti CF. Pathology of multiple sclerosis: Where do we stand? *Continuum (Minneapolis)*. 2013;19(4 Multiple Sclerosis):901–921.

45. Angermueller C, Parnamaa T, Parts L, Stegle O. Deep learning for computational biology. *Mol Syst Biol.* 2016;12(7):878-
46. Zhang GP. Neural networks for classification: A survey. *IEEE Trans Syst Man Cybern Part C Appl Rev.* 2000;30(4):451–462.
47. Zivadinov R, Horakova D, Bergsland N, et al. A serial 10-year follow-up study of atrophied brain lesion volume and disability progression in patients with relapsing-remitting MS. *AJNR Am J Neuroradiol.* 2019;40(3):446–452.
48. Genovese AV, Hagemeyer J, Bergsland N, et al. Atrophied brain T2 lesion volume at MRI is associated with disability progression and conversion to secondary progressive multiple sclerosis. *Radiology.* 2019;293(2):424–433.
49. Maranzano J, Dadar M, Rudko DA, et al. Comparison of multiple sclerosis cortical lesion types detected by multicontrast 3T and 7T MRI. *AJNR Am J Neuroradiol.* 2019;40(7):1162–1169.
50. Metz I, Weigand SD, Popescu BF, et al. Pathologic heterogeneity persists in early active multiple sclerosis lesions. *Ann Neurol.* 2014;75(5):728–738.
51. Absinta M, Sati P, Gaitan MI, et al. Seven-tesla phase imaging of acute multiple sclerosis lesions: A new window into the inflammatory process. *Ann Neurol.* 2013;74(5):669–678.
52. Beck ES, Sati P, Sethi V, et al. Improved visualization of cortical lesions in multiple sclerosis using 7T MP2RAGE. *AJNR Am J Neuroradiol.* 2018;39(3):459–466.
53. Louapre C, Govindarajan ST, Gianni C, et al. Beyond focal cortical lesions in MS: An in vivo quantitative and spatial imaging study at 7T. *Neurology.* 2015;85(19):1702–1709.
54. Muccilli A, Seyman E, Oh J. Spinal cord MRI in multiple sclerosis. *Neurol Clin.* 2018;36(1):35–57.